

## Electronic Supplementary Information

### Regulate Microenvironment of $\text{Pb}_2\text{O}_3@\text{Bi}_2\text{O}_3$ -Tube by Structural Reconstruction for Boosting the Electrochemical Ozone Production Performance

*Huaijie Shi<sup>a</sup>, Xiaosa Wang<sup>a</sup>, Xiaoge Peng<sup>a</sup>, Mingzhe Xue<sup>a</sup>, Yufeng Xue<sup>a</sup>,  
Fengying Gao<sup>a</sup>, Xing Zhong<sup>a b \*</sup>, Jianguo Wang<sup>a \*</sup>*

<sup>a</sup> Institute of Industrial Catalysis, State Key Laboratory Breeding Base of Green-Chemical Synthesis Technology, College of Chemical Engineering, Zhejiang University of Technology, Hangzhou 310032, P.R. China.

<sup>b</sup> Innovation Research Center for Advanced Environmental Technology Eco-industrial Innovation Institute ZJUT, Rong-chang East Road, Quzhou, 324400, China

\*Correspondence and requests for materials should be addressed to X. Z. (email: zhongx@zjut.edu.cn), J. G. W. (email: jgw@zjut.edu.cn).

---

## Supplementary Results

### Experimental Reagents and Conditions.

**Figure S1.** The SEM image of (a) Bi<sub>2</sub>O<sub>3</sub>-alkali and (b) Bi<sub>2</sub>O<sub>3</sub>-acid.

**Figure S2.** Bi<sub>2</sub>O<sub>3</sub>-Tube intermediates obtained at different reaction times (a: 5 min; b: 20 min; c: 40 min; d: 60 min).

**Figure S3.** The SEM image of Pb<sub>2</sub>O<sub>3</sub>/Bi<sub>2</sub>O<sub>3</sub>-Commercial.

**Figure S4.** The XRD pattern of Bi<sub>2</sub>O<sub>3</sub>-Commercial and Pb<sub>2</sub>O<sub>3</sub>/Bi<sub>2</sub>O<sub>3</sub>-Commercial.

**Figure S5.** The XPS full spectrum of (a) Bi<sub>2</sub>O<sub>3</sub>-Commercial, (b) Bi<sub>2</sub>O<sub>3</sub>-Tube, (c) Pb<sub>2</sub>O<sub>3</sub>/Bi<sub>2</sub>O<sub>3</sub>-Commercial, and (d) Pb<sub>2</sub>O<sub>3</sub>@Bi<sub>2</sub>O<sub>3</sub>-Tube.

**Figure S6.** High-resolution Bi 4f XPS spectra of Bi<sub>2</sub>O<sub>3</sub>-Commercial and Pb<sub>2</sub>O<sub>3</sub>/Bi<sub>2</sub>O<sub>3</sub>-Commercial.

**Figure S7.** High-resolution Pb 4f XPS spectra of Pb<sub>2</sub>O<sub>3</sub>/Bi<sub>2</sub>O<sub>3</sub>-Commercial and Pb<sub>2</sub>O<sub>3</sub>.

**Figure S8.** High-resolution O 1s XPS spectra of Bi<sub>2</sub>O<sub>3</sub>-Commercial and Pb<sub>2</sub>O<sub>3</sub>/Bi<sub>2</sub>O<sub>3</sub>-Commercial.

**Figure S9.** The EPR pattern of Pb<sub>2</sub>O<sub>3</sub>@Bi<sub>2</sub>O<sub>3</sub>-Tube.

**Figure S10.** The LSV curves before and after stability test.

**Figure S11.** The CV curves at different scan rates (20, 40, 60, 80, 100, and 120 mV/s) in the region of 1.21-1.31 V vs.RHE of (a) Bi<sub>2</sub>O<sub>3</sub>-Commercial, (b) Pb<sub>2</sub>O<sub>3</sub>/Bi<sub>2</sub>O<sub>3</sub>-Commercial, (c) Bi<sub>2</sub>O<sub>3</sub>-Tube, and (d) Pb<sub>2</sub>O<sub>3</sub>@Bi<sub>2</sub>O<sub>3</sub>-Tube.

**Figure S12.** The color change of ozone detection powder with electrolyte after reacting for different electrocatalysts.

**Figure S13.** The standard curve of ozonated water concentration in saturated K<sub>2</sub>SO<sub>4</sub> solution

**Figure S14.** The colorimetric reaction of moist starch potassium iodide test paper with

---

gaseous ozone produced by different electrocatalysts (a: Bi<sub>2</sub>O<sub>3</sub>-Commercial; b: Pb<sub>2</sub>O<sub>3</sub>/Bi<sub>2</sub>O<sub>3</sub>-Commercial; c: Bi<sub>2</sub>O<sub>3</sub>-Tube; d: Pb<sub>2</sub>O<sub>3</sub>@Bi<sub>2</sub>O<sub>3</sub>-Tube).

**Figure S15.** The concentrations of gaseous ozone produced by different electrocatalysts at different times.

**Figure S16.** The EPR pattern of Pb<sub>2</sub>O<sub>3</sub>@Bi<sub>2</sub>O<sub>3</sub>-Tube Before and After EOP test.

**Figure S17.** (a) Electrocatalytic degradation curves of p-Nitrophenol at different current density and (b) corresponding pseudo-first-order kinetic fitting results.

**Figure S18.** (a) Electrocatalytic degradation curves of p-Nitrophenol at different pH and (b) corresponding pseudo-first-order kinetic fitting results.

**Figure S19.** (a) Electrocatalytic degradation curves of p-Nitrophenol at different electrocatalyst loads and (b) corresponding pseudo-first-order kinetic fitting results.

**Figure S20.** (a) Electrocatalytic degradation curves of p-Nitrophenol at different electrolyte temperature and (b) corresponding pseudo-first-order kinetic fitting results.

**Figure S21.** The HPLC pattern of (a) formic acid, (b) 1, 4-benzoquinone, (c) catechol, (d) Phenol, (e) Phloroglucinol, (f) hydroquinone.

**Table. S1** Elemental compositions of Pb<sub>2</sub>O<sub>3</sub>@Bi<sub>2</sub>O<sub>3</sub>-Tube and Pb<sub>2</sub>O<sub>3</sub>/Bi<sub>2</sub>O<sub>3</sub>-Commercial by ICP-MS for Pb and Bi content.

**Table. S2** The content and position of Oxygen Vacancy for the prepared electrocatalysts.

**Table. S3** The performance comparison of Pb<sub>2</sub>O<sub>3</sub>@Bi<sub>2</sub>O<sub>3</sub>-Tube with other electrocatalysts toward for EOP.

**Table. S4** The content of Pb and Bi for the electrolyte and electrocatalysts after EOP test.

**Table. S5** The reaction rate constant of quenching agents with ROS.

---

## Experimental Reagents and Conditions.

Bi(NO<sub>3</sub>)<sub>3</sub>·5H<sub>2</sub>O (99.0%, Macklin Biochemical Co., Ltd.), HNO<sub>3</sub> (Macklin Biochemical Co., Ltd.), Pb(NO<sub>3</sub>)<sub>2</sub>·5H<sub>2</sub>O (99.0%, Macklin Biochemical Co., Ltd.), NaOH (Macklin Biochemical Co., Ltd.), NaClO (≥5 %, Shanghai Lingfeng Reagent Co., Ltd.), K<sub>2</sub>SO<sub>4</sub> (99.0%, Aladdin Industrial Co., Ltd.), Ti felts (Zhejiang Jiuyu Technology Co., Ltd), Nafion (5.0-5.4 wt%, Suzhou Yilongcheng Energy Technology Co., Ltd.), H<sub>3</sub>PO<sub>4</sub> (AR, Sinopharm Chemical Reagent Co., Ltd.), ethanol (≥99.7%; Sinopharm Chemical Reagent Co., Ltd.), indigotindisulfonate sodium (96%, Aladdin Industrial Co., Ltd.), starch iodide paper (Shanghai Sanaisi Reagent Co., Ltd.), I<sub>2</sub> (99%; Aladdin Industrial Co., Ltd.), p-nitrophenol (99%, Aladdin Industrial Co., Ltd.), Na<sub>2</sub>S<sub>2</sub>O<sub>3</sub> (≥99.0%, Sinopharm Chemical Reagent Co., Ltd.), Tert-Butanol (99%, Macklin Biochemical Co., Ltd.), L- histidine (≥99.0%, Aladdin Industrial Co., Ltd.), formic acid (99 %, Macklin Biochemical Co., Ltd.), p-benzoquinone (≥99.0%, Aladdin Industrial Co., Ltd.), phenol (99 %, Aladdin Industrial Co., Ltd.), Phloroglucinol (99.0%, Aladdin Industrial Co., Ltd.), catechol (99 %, Aladdin Industrial Co., Ltd.), Millipore deionized water were used to prepare all the solutions.

Bi<sub>2</sub>O<sub>3</sub>-Tube was prepared through the wet chemical synthesis. Firstly, the 0.97 g bismuth nitrate was dissolved in 15% nitric acid (15 mL), then added 40 mL deionized water and stirred at 70°C for 1h. Then the 20 mL NaOH (16%) solution was added to the mixture and continue stirring for 1 h. After natural cooling to room temperature, filter and dry to obtain Bi<sub>2</sub>O<sub>3</sub>-Tube. Afterwards, 90 mg of Bi<sub>2</sub>O<sub>3</sub>-Tube and 14 mg of Pb(NO<sub>3</sub>)<sub>2</sub> was dispersed in 1 M NaOH solution (20 mL) for stirring and heating for 30 min at 60 °C , then the 3 mL NaClO (the effective chlorine content was 5-14 %) was added to the mixture and maintained at 90°C for 6 h. Afterwards, the obtained powder was washed three times with anhydrous ethanol and deionized water and named as Pb<sub>2</sub>O<sub>3</sub>@Bi<sub>2</sub>O<sub>3</sub>-Tube.

In order to fully characterize the prepared catalysts, a variety of techniques were employed. Scanning electron microscope (SEM) images were obtained through Hitachi FE-SEM S-4700. X-ray diffraction (XRD) technique was used to receive the phase of the prepared electrocatalysts by Bruker D8 Advance powder X-ray Co Ka radiation diffractometer and operating at 40 kV and 40 mA. Surface analysis was performed using a Thermo Scientific K-Alpha X-Ray Photoelectron Spectrometer (XPS) equipped with an Al K-alpha source (hν=1486.6 eV). The core-level spectra of elements were calibrated using the C1s peak, which was adjusted to 284.80 eV. The electrocatalyst vacancies was determinate by Bruker EMXplus-6/1.

All electrochemical measurements were performed by CHI 760E electrochemical workstation using standard three-electrode system. The prepared electrocatalyst (8.0 mg), anhydrous ethanol (900 μL) and Nafion solution (100 μL) were mixed and followed by ultrasound for 30 min to acquired homogeneous ink solution. Then, the mixture was spread on Ti felts (2\*2 cm) to prepare a working electrode (WE). The Pt plate and Ag/AgCl

electrode were used as the counter electrode (CE) and reference electrode (RE), and the saturated K<sub>2</sub>SO<sub>4</sub> solution was used electrolyte. The measured potentials vs. Ag/AgCl were converted to potentials relative to the reversible hydrogen electrode (RHE) according to the followed equation:  $E_{\text{RHE}} = E_{\text{Ag/AgCl}} + 0.197 \text{ V} + 0.059 \times \text{pH}$ . Cyclic voltammetry (CV) and polarization curves analysis were performed to prove the electrochemical activity of the prepared electrocatalysts toward EOP. The polarization curve was performed at a sweeping rate of 5 mV/s. The electrochemical double layer capacitance ( $C_{\text{dl}}$ ) was determined from the CV curves at different scan rates (20-120 mV/s) in nonreactive region according to the equation:  $C_{\text{dl}} = I_c/v$ , where  $v$ ,  $I_c$ , and  $C_{\text{dl}}$  were the scan rate, charging current, and the double-layer capacitance of the electro-active materials, respectively. EIS measurements were carried out from 0.1 to 100,000 Hz with an amplitude of 10 mV at 2.0 V.

The quantitative and qualitative tests of gaseous ozone and ozonated water were measured through amperostat. The Pt plate were used as the RE, and prepared electrocatalyst was used as the WE. For the qualitative determination of ozonated water, the continuous current response of 50 mA cm<sup>-2</sup> was provided for 10 min. Subsequently, the reacted electrolyte was mixed with ozone detection powder and left for 3 min to observe the color change. The higher the ozonated water concentration, the darker the color of the mixture. The concentration of ozonated water was quantitative determined by Indigo disulphonate spectrophotometry (IDS) method. Firstly, the standard curve was plotted by follows: a mixture of H<sub>3</sub>PO<sub>4</sub>-NaH<sub>2</sub>PO<sub>2</sub> at pH = 2.0 (10 mL and) and 0, 2, 4, 6, and 8 mL of O<sub>3</sub>-saturated solution were added to a 25 mL glass bottle, respectively. And 14.25 mL saturated K<sub>2</sub>SO<sub>4</sub> solution and 0.75 mL indigo carmine solution (1 mM) were added to each flask, respectively. After 3 min, the absorbance of the above solution was measured at 610 nm using a UV-visible spectrophotometer (SP-752PC) and a blank solution was used for background correction. Corresponding, the standard curve was obtained by the relations between absorbance and ozone concentration. The solution after EOP test (14.25 mL), 1 mM indigo buffer solution (0.75 mL), and pH = 2.0 H<sub>3</sub>PO<sub>4</sub>-NaH<sub>2</sub>PO<sub>2</sub> (10 mL) were added to a volumetric flask and allowed to stand for 3 min. And the absorbance of mixture was acquired at 610 nm by UV-visible spectrophotometer, thus the concentration of the ozonated water to be measured could be obtained by comparing the standard curve.

The iodized starch papers placing over the working electrode were used in determining ozonated gas as indicator in order to qualitative determine the gaseous ozone. With the running time increased, the test paper gradually changed to darker color. And the darker the color was, the higher ozonated gas concentration was. The 2B ozone monitor was used to be qualitatively measured the concentration of gaseous ozone. And the FE<sub>O<sub>3</sub></sub>(%) was calculated as follows:

$$FE_{O_3} = \frac{5 * F * Q}{3 * M_{O_3} * I} \times 100$$

---

where  $I$  was current (A), and  $M_{O_3}$  was molecular weight of  $O_3$  (48),  $Q$  was ozone production rate (kg/h), and  $F$  was Faraday's constant (96485 C/mol).

The electrodegradation of p-nitrophenol was carried out through two-electrode system. The Pt sheet was CE, the  $Pb_2O_3@Bi_2O_3$ -Tube was WE, and the saturated potassium sulfate with 50 mg p-nitrophenol was electrolyte. The concentrations of intermediate products were analyzed by using a high-performance liquid chromatography (HPLC). The free radicals produced during the reaction were obtained by ESR test. The main reactive oxygen species produced in the reaction process were detected by 2, 2, 6, 6-tetramethylpiperidine (TEMP) and 5, 5-dimethyl-1-oxypyrroline (DMPO) as the trapping agent. For the p-nitrophenol, the mobile phase was a mixture of methyl alcohol and water containing 0.05% acetic acid in a 1:1 ratio, the flow rate was  $1 \text{ mL min}^{-1}$ , and the detection wavelength was 287 nm.

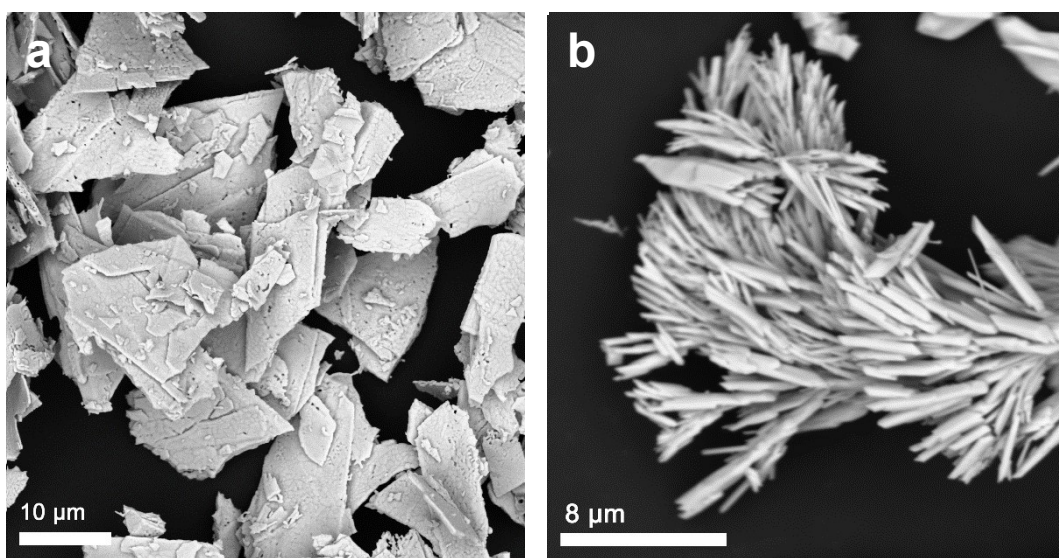


**Figure S1.** The SEM image of (a) Bi<sub>2</sub>O<sub>3</sub>-alkali and (b) Bi<sub>2</sub>O<sub>3</sub>-acid.

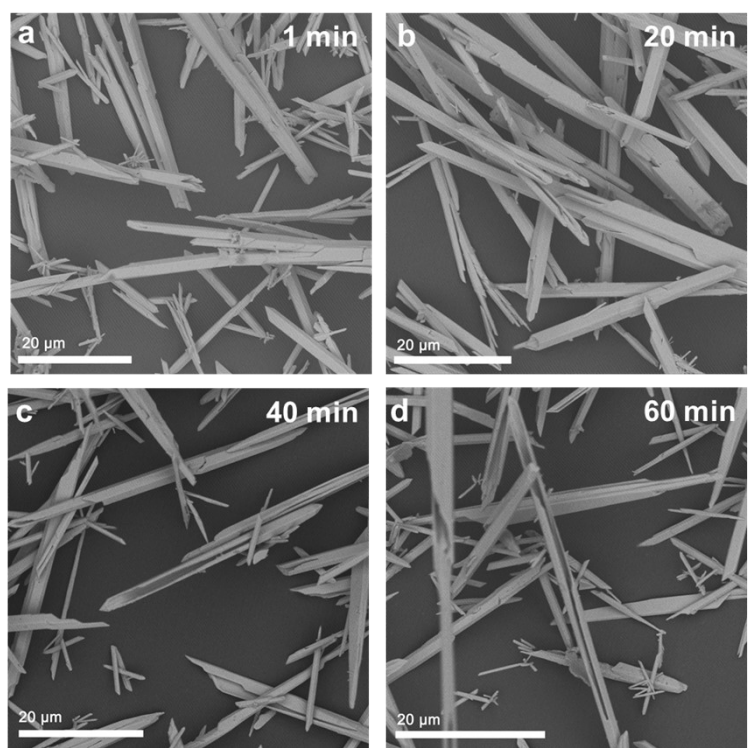


**Figure S2.** Bi<sub>2</sub>O<sub>3</sub>-Tube intermediates obtained at different reaction times (a: 5 min; b: 20 min; c: 40 min; d: 60 min)

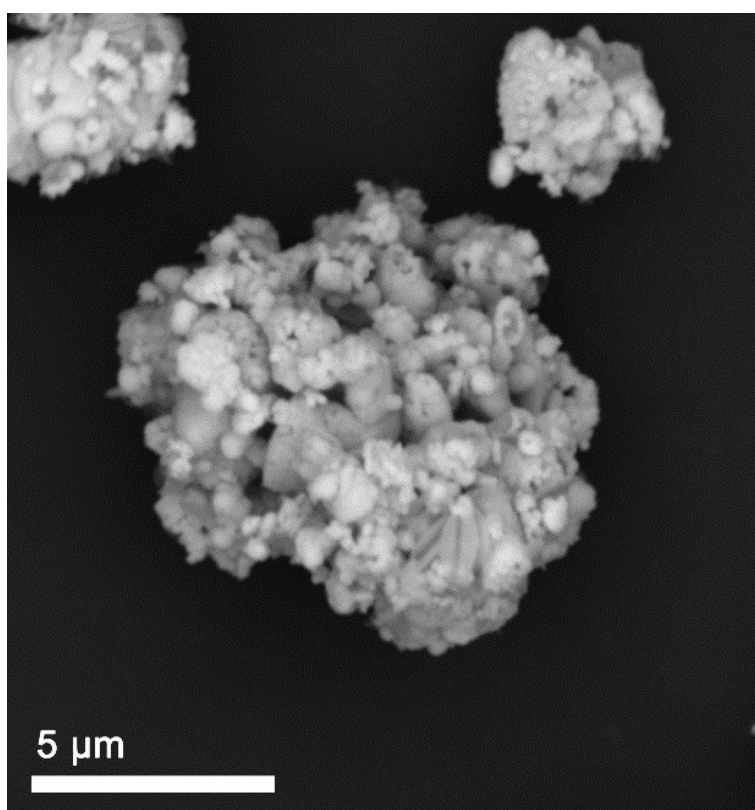


**Figure S3.** The SEM image of  $\text{Pb}_2\text{O}_3/\text{Bi}_2\text{O}_3$ -Commercial.

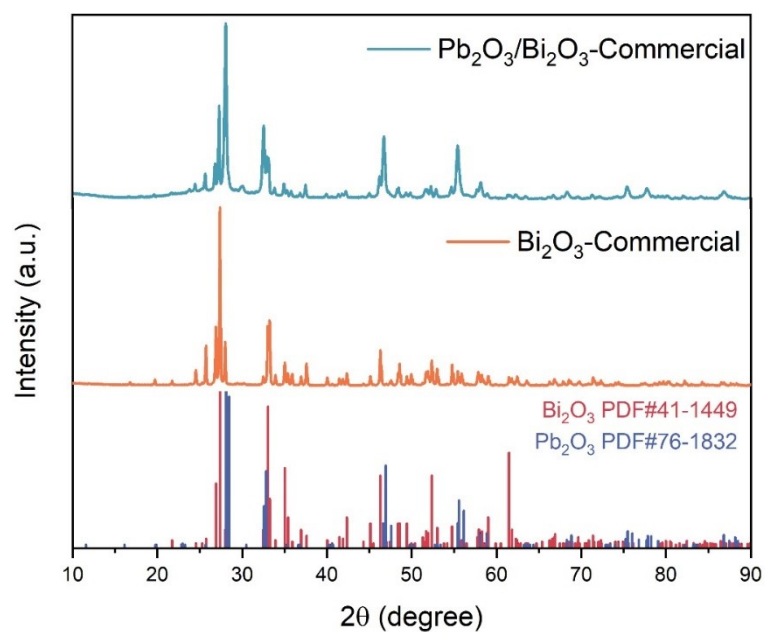


**Figure S4.** The XRD pattern of Bi<sub>2</sub>O<sub>3</sub>-Commercial and Pb<sub>2</sub>O<sub>3</sub>/Bi<sub>2</sub>O<sub>3</sub>-Commercial.

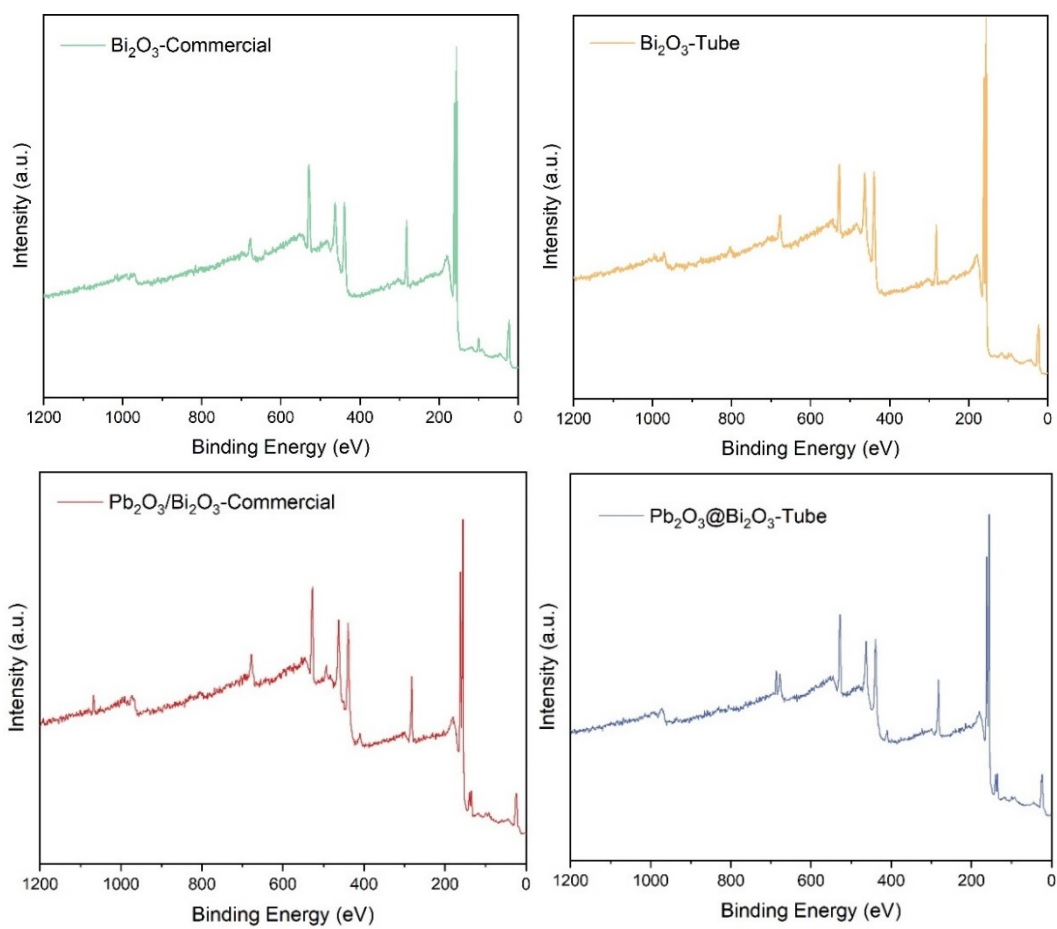


**Figure S5.** The XPS full spectrum of (a)  $\text{Bi}_2\text{O}_3$ -Commercial, (b)  $\text{Bi}_2\text{O}_3$ -Tube, (c)  $\text{Pb}_2\text{O}_3/\text{Bi}_2\text{O}_3$ -Commercial, and (d)  $\text{Pb}_2\text{O}_3@\text{Bi}_2\text{O}_3$ -Tube.

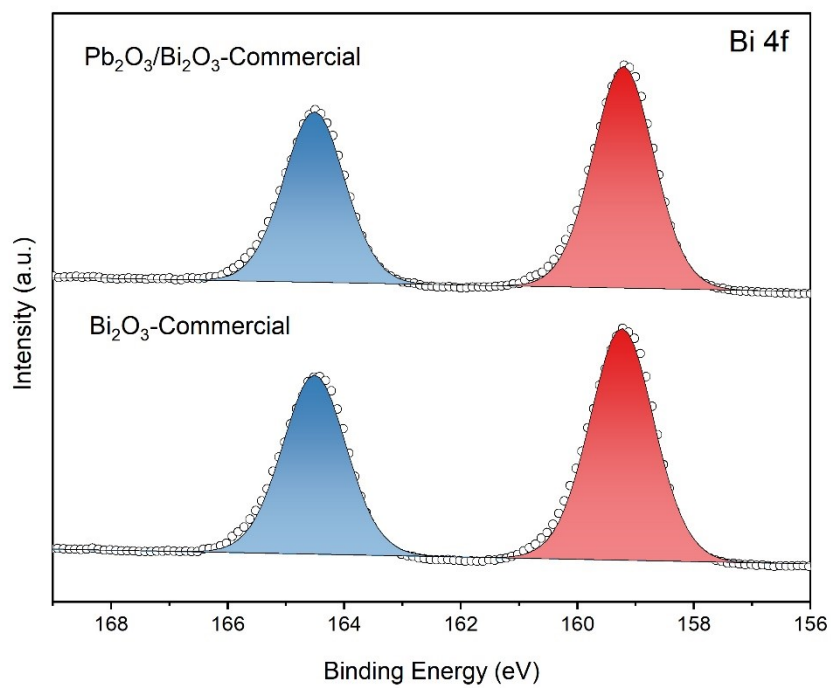


**Figure S6.** High-resolution Bi 4f XPS spectra of  $\text{Pb}_2\text{O}_3/\text{Bi}_2\text{O}_3$ -Commercial and  $\text{Bi}_2\text{O}_3$ -Commercial.

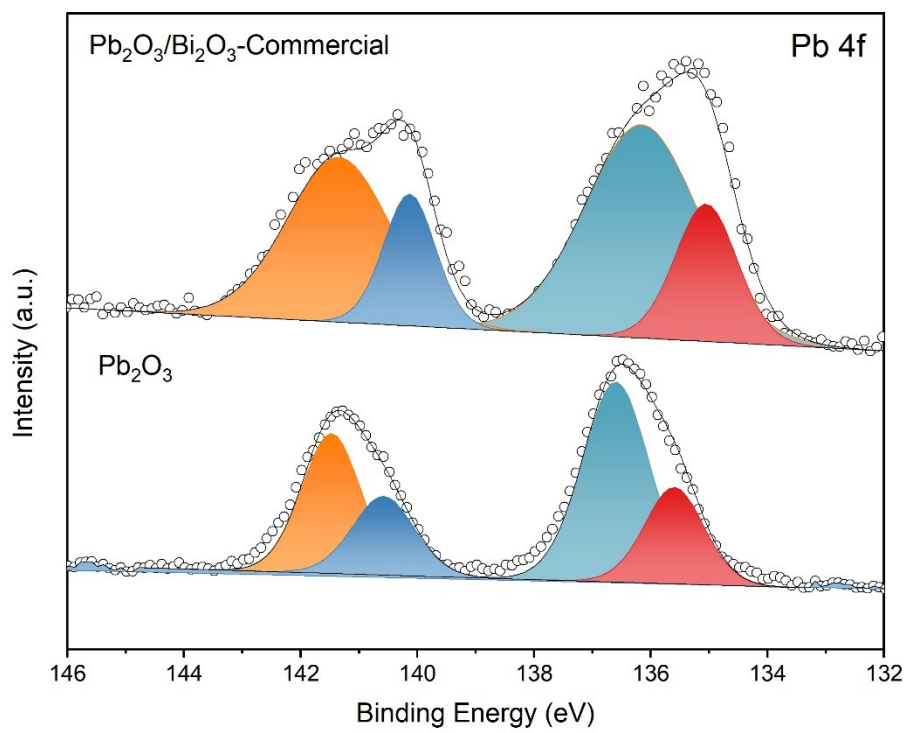


**Figure S7.** High-resolution Pb 4f XPS spectra of Pb<sub>2</sub>O<sub>3</sub>/Bi<sub>2</sub>O<sub>3</sub>-Commercial and Pb<sub>2</sub>O<sub>3</sub>.

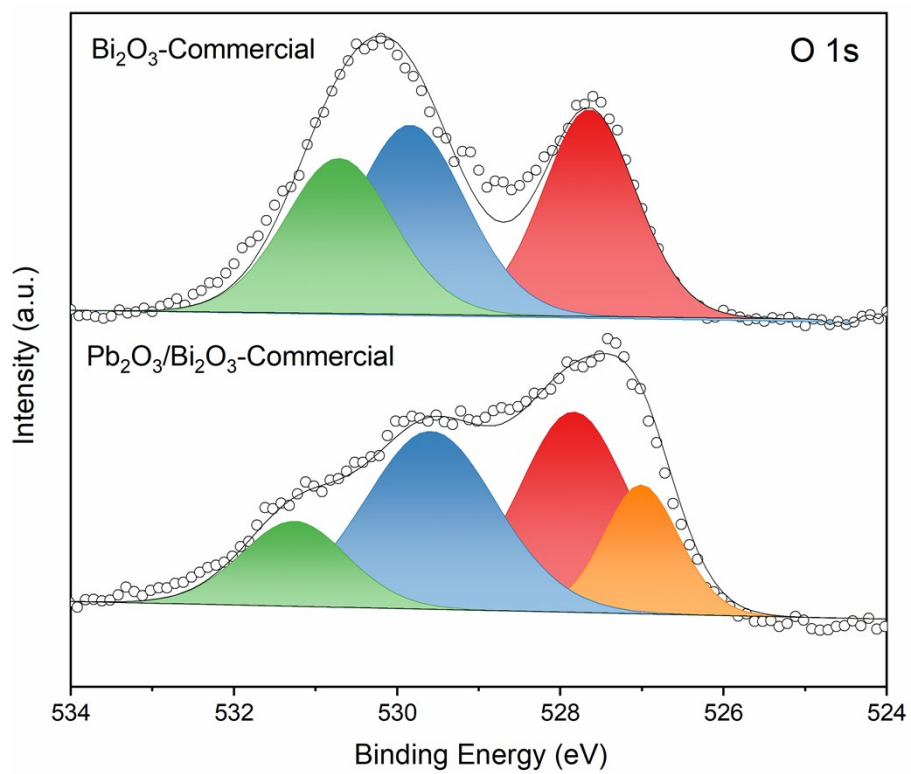


**Figure S8.** High-resolution O 1s XPS spectra of Bi<sub>2</sub>O<sub>3</sub>-Commercial and Pb<sub>2</sub>O<sub>3</sub>/Bi<sub>2</sub>O<sub>3</sub>-Commercial.

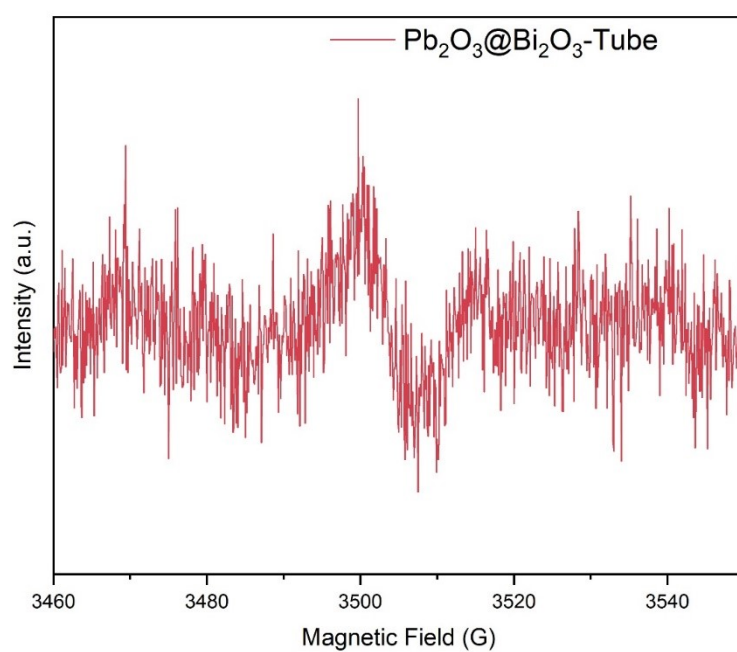


**Figure S9.** The EPR pattern of  $\text{Pb}_2\text{O}_3@ \text{Bi}_2\text{O}_3\text{-Tube}$ .

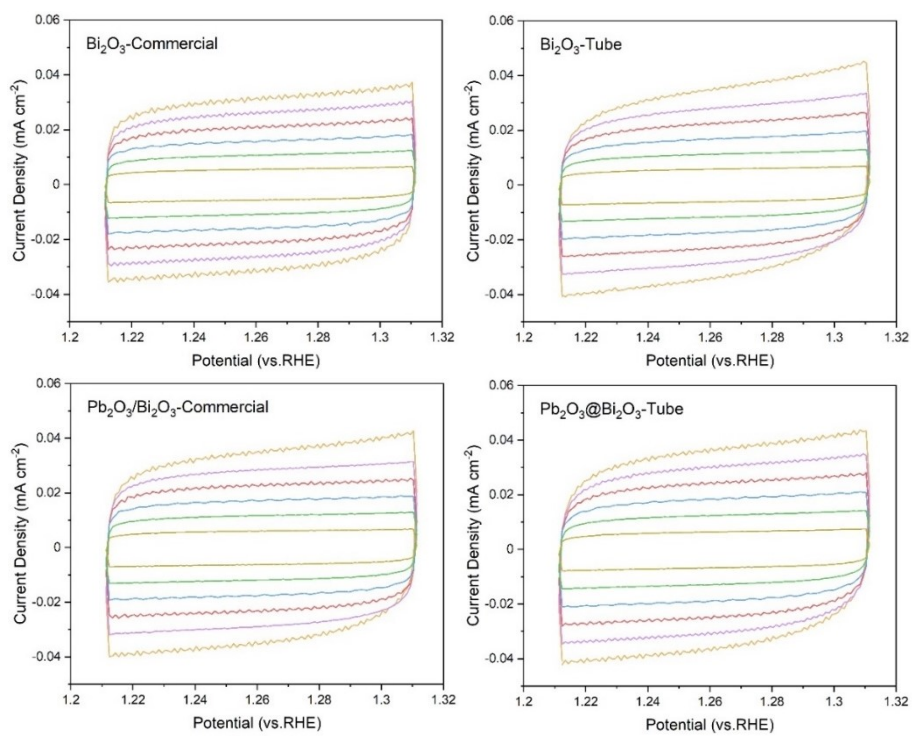


**Figure S10.** The CV curves at different scan rates (20, 40, 60, 80, 100, and 120 mV/s) in the region of 1.21-1.31 V vs.RHE of (a) Bi<sub>2</sub>O<sub>3</sub>-Commercial, (b) Bi<sub>2</sub>O<sub>3</sub>-Tube, (c) Pb<sub>2</sub>O<sub>3</sub>/Bi<sub>2</sub>O<sub>3</sub>-Commercial, and (d) Pb<sub>2</sub>O<sub>3</sub>@Bi<sub>2</sub>O<sub>3</sub>-Tube.

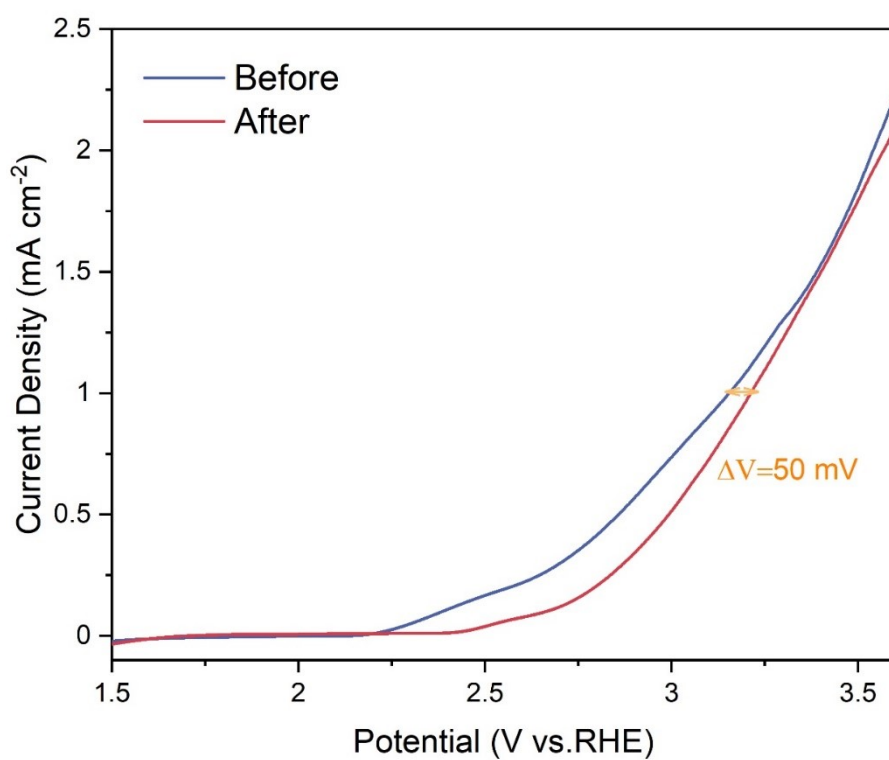


**Figure S11.** The LSV curves before and after stability test.

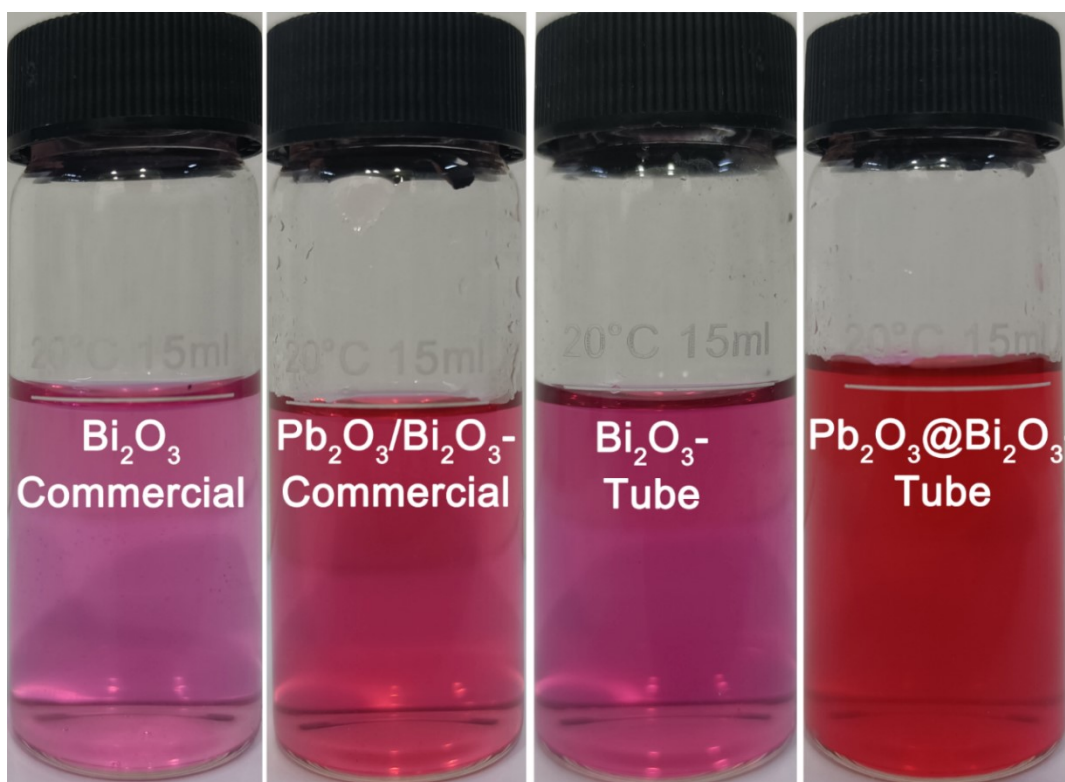


**Figure S12.** The color change of ozone detection powder with electrolyte after reacting for different electrocatalysts.

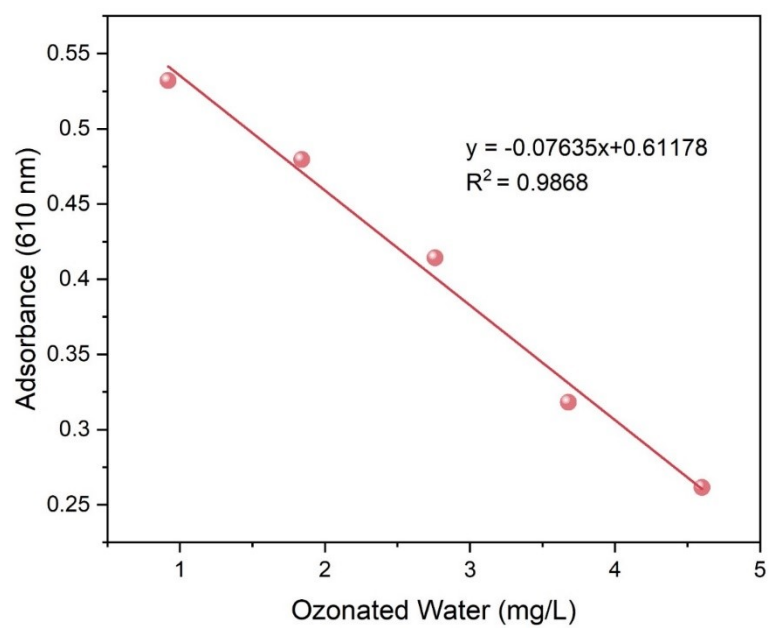


**Figure S13.** The standard curve of ozonated water concentration in saturated  $K_2SO_4$  solution

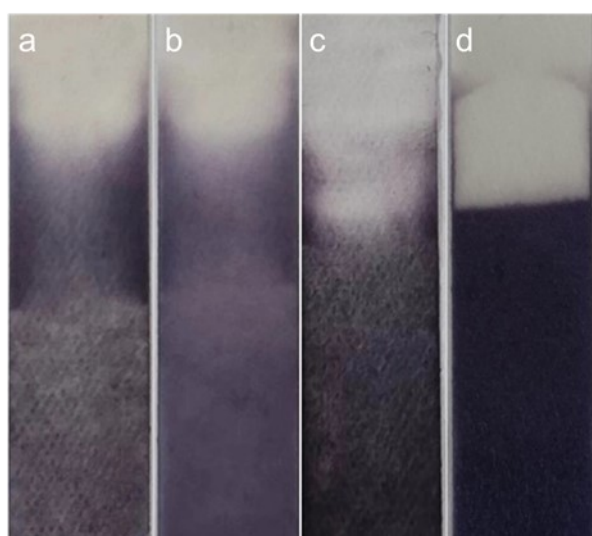


**Figure S14.** The colorimetric reaction of moist starch potassium iodide test paper with gaseous ozone produced by different electrocatalysts (a:  $\text{Bi}_2\text{O}_3$ -Commercial; b:  $\text{Pb}_2\text{O}_3/\text{Bi}_2\text{O}_3$ -Commercial; c:  $\text{Bi}_2\text{O}_3$ -Tube; d:  $\text{Pb}_2\text{O}_3@\text{Bi}_2\text{O}_3$ -Tube).

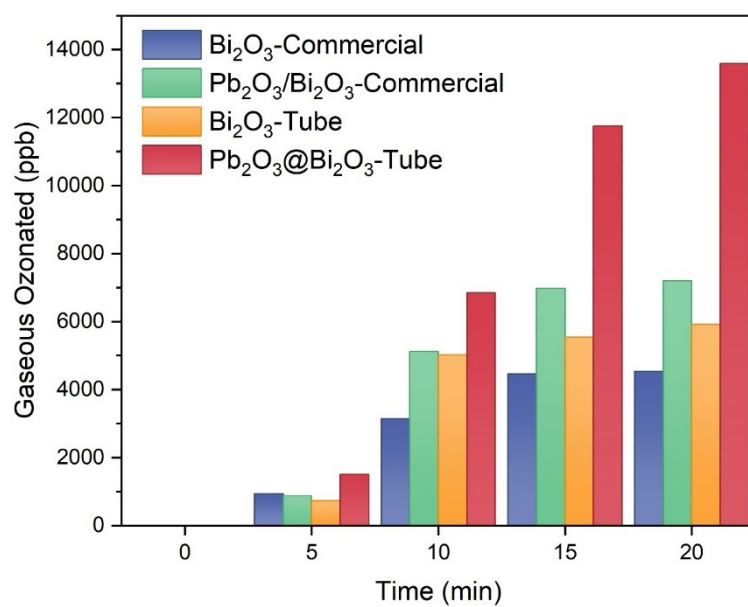


**Figure S15.** The concentrations of gaseous ozone produced by different electrocatalysts at different times.

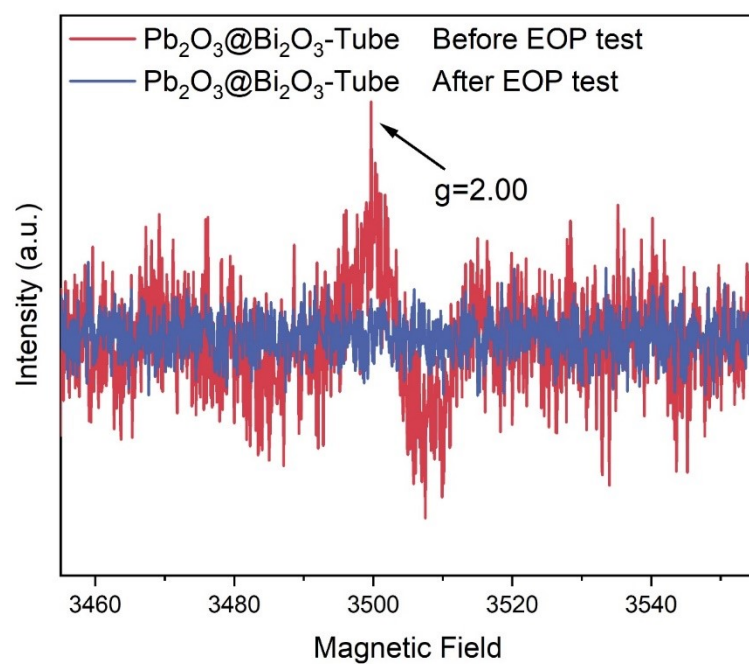


**Figure. S16.** The EPR pattern of  $\text{Pb}_2\text{O}_3@ \text{Bi}_2\text{O}_3$ -Tube Before and After EOP test.

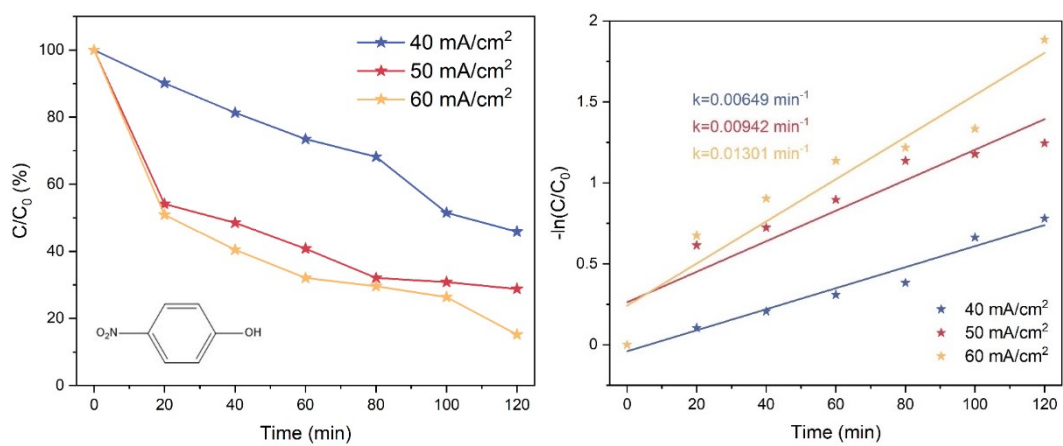


**Figure S17.** (a) Electrocatalytic degradation curves of p-Nitrophenol at different current density and (b) corresponding pseudo-first-order kinetic fitting results.

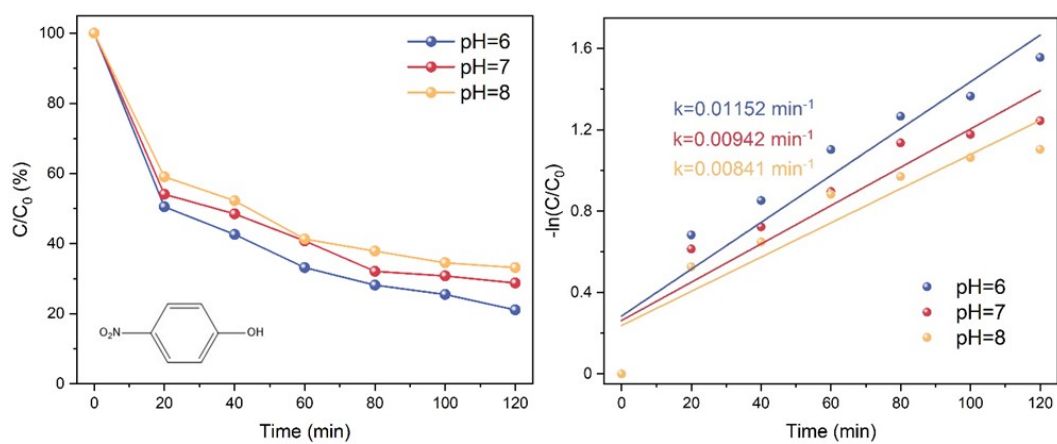


**Figure S18.** (a) Electrochemical degradation curves of p-Nitrophenol at different pH and (b) corresponding pseudo-first-order kinetic fitting results.

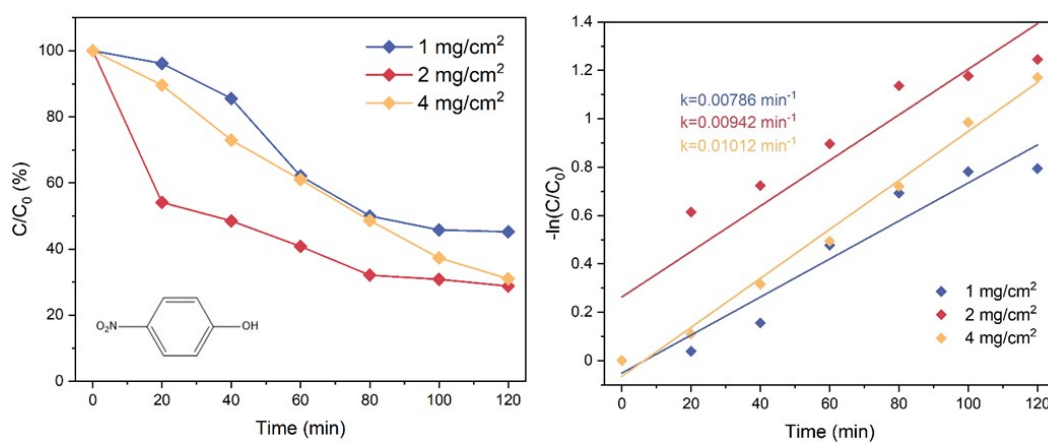


**Figure S19.** (a) Electrocatalytic degradation curves of p-Nitrophenol at different electrocatalyst loads and (b) corresponding pseudo-first-order kinetic fitting results.

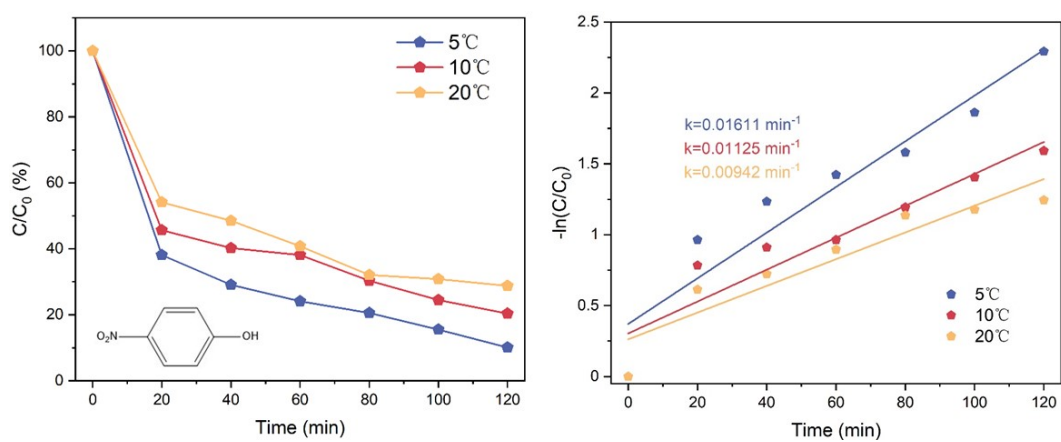


**Figure S20.** (a) Electrocatalytic degradation curves of p-Nitrophenol at different electrolyte temperature and (b) corresponding pseudo-first-order kinetic fitting results.

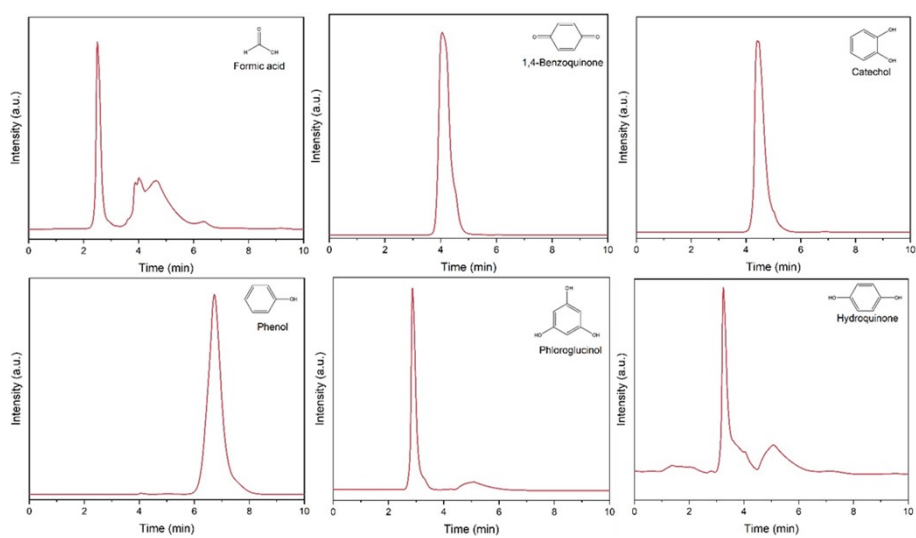


**Figure S21.** The HPLC pattern of (a) formic acid, (b) 1, 4-benzoquinone, (c) catechol, (d) Phenol, (e) Phloroglucinol, (f) hydroquinone.

---

**Table S1.** Elemental compositions of  $\text{Pb}_2\text{O}_3@\text{Bi}_2\text{O}_3$ -Tube and  $\text{Pb}_2\text{O}_3/\text{Bi}_2\text{O}_3$ -Commercial by ICP-MS for Pb and Bi content

<b>Samples</b>	<b>Pb loading (%)</b>	<b>Bi loading (%)</b>
$\text{Pb}_2\text{O}_3@\text{Bi}_2\text{O}_3$ -Tube	9.11%	80.10%
$\text{Pb}_2\text{O}_3/\text{Bi}_2\text{O}_3$ -Commercial	8.94%	79.10%

---

**Table S2.** The content and position of Oxygen Vacancy for the prepared electrocatalysts.

<b>Samples</b>	<b>Position</b>	<b>The Content of Oxygen Vacancy</b>
Pb <sub>2</sub> O <sub>3</sub>	529.57 eV	38.04 %
Bi <sub>2</sub> O <sub>3</sub> -Commercial	529.61 eV	35.57 %
Pb <sub>2</sub> O <sub>3</sub> /Bi <sub>2</sub> O <sub>3</sub> -Commercial	529.47 eV	36.84 %
Bi <sub>2</sub> O <sub>3</sub> -Tube	529.40 eV	36.18 %
Pb <sub>2</sub> O <sub>3</sub> @Bi <sub>2</sub> O <sub>3</sub> -Tube	529.60 eV	45.30 %

---

**Table. S3** The performance comparison of  $\text{Pb}_2\text{O}_3@\text{Bi}_2\text{O}_3$ -Tube with other electrocatalysts toward for EOP.

Electrocatalysts	$\text{FE}_{\text{O}_3}$	Ref.
<b><math>\text{Pb}_2\text{O}_3@\text{Bi}_2\text{O}_3</math>-Tube</b>	<b>11.29%</b>	<b>This work</b>
Pt-TaO <sub>x</sub> /Ti	11.7%	Electrochem. Commun. 8, 1263-1269 (2006)
ZnO/ZnS@C-750	10.8%	J. Mater. Chem. A,2023, 11,3454–3463
OFM-Fe-PbO <sub>2</sub>	10%	J. Environ. Chem. Eng., 2016, 4, 418-427
Si/TiO <sub>x</sub> /Pt/TiO <sub>2</sub>	9%	J. Electrochem. Soc. 157, F30 (2010).
PtZn/Zn-N-C	4.2%	J. Energy Chem. 51, 312 322 (2020)
D-BNC	1.7%	J. Mater. Chem. A, 2020,8, 2336-2342

---

**Table. S4** The content of Pb and Bi for the electrolyte and electrocatalysts after EOP test.

<b>Samples</b>	<b>The content of Bi</b>	<b>The content of Pb</b>
The electrolyte after EOP test	0.426 ppm	0.104 ppm
The electrocatalysts after EOP test	87.85 %	8.81 %

---

**Table. S5** The reaction rate constant of quenching agents with ROS.

Quenching agents	First order reaction rate constant (s <sup>-1</sup> )		
	<sup>1</sup> O <sub>2</sub>	·O <sub>2</sub> <sup>-</sup>	·OH
TBA	<5 × 10 <sup>3</sup>	<5 × 10 <sup>2</sup>	3.8 × 10 <sup>8</sup>
p-benzoquinone	3.8 × 10 <sup>4</sup>	1.0 × 10 <sup>6</sup>	1.2 × 10 <sup>6</sup>
L-histidine	1.32 × 10 <sup>5</sup>	<2 × 10 <sup>-3</sup>	1.0 × 10 <sup>7</sup>

---